

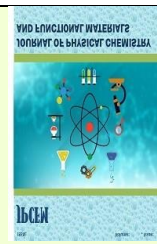
## PAPER DETAILS

TITLE: Isotopic Effect on The Quantum Dynamics of ND+H/ NT+H Reaction

AUTHORS: Seda HEKIM

PAGES: 59-65

ORIGINAL PDF URL: <https://dergipark.org.tr/tr/download/article-file/887404>



## Isotopic Effect on the Quantum Dynamics of ND+H NT+H Reactions

 Seda Hekim<sup>a</sup>
<sup>a</sup>Department of Physics, Faculty of Science, Firat University, 23169 Elazig Turkey

## ABSTRACT

The time-dependent wave packet method was employed to study the ND+H and NT+H reactions on the modified NH<sub>2</sub> potential energy surface (PES) for  $\tilde{A}^2 A_1$  excited state. All the calculations are carried out using Centrifugal Sudden approximation method. So, reaction kinetics were obtained for different initial rotation quantum numbers. The role of intermolecular isotope effects on reaction kinetics was emphasized.

## ARTICLE INFO

## Keywords:

Reaction kinetics  
Centrifugal Sudden approximation,  
Isotope effects

Revised: 05-December-2019

Accepted: 09-December-2019

ISSN: 2651-3080

## 1. Introduction

Chemical reactions involving NH and NH<sub>2</sub> play an important role in the imidogen (NH) degradation in the gas phase combustion reactions, atmospheric, and interstellar systems. Thus, the nitrogen atom reactions, particularly with hydrogen, have received considerable attention lately.

Isotopic variants play an important role in molecular reaction dynamics. It is known that the NH+H reaction and isotopic variant systems have contribution to the quality of the atmospheric environment, so the studies in this aspect have attracted the attention of scientific researches. So, the H + NH reaction and its isotopic variations have been the subject of many experimental measurements and theoretical studies. Although the NH + H reaction and isotopic variant reaction attracted great attention, little information is known about the dynamics of the T isotopic variable reaction. Experimentally, the dynamics of the N + H<sub>2</sub> reaction were investigated by different groups [1-3]. Suzuki et. al. obtained the temperature-dependent rate constants of the reactions of N(<sup>2</sup>D) with H<sub>2</sub> and D<sub>2</sub> [4]. The rate constants for reactions NH+H and NH+D were determined in a quasi-static- laser- flash photolysis at room temperature [5, 6]. From the theoretical side, both classical and quantum dynamics studies have been conducted for the NH<sub>2</sub> reaction

systems [5-25]. The global potential energy surfaces for the ground state of the NH<sub>2</sub> (<sup>4</sup>A'') and NHD (<sup>2</sup>A'') systems have been constructed by Adam et al. using the multireference configuration interaction (MRCI) method and the augmented correlation consistent polarized valence quadruple zeta (aug-cc-pVQZ) basis set [5, 6]. Then the same group has calculated the reaction kinetics with a quasi-classical trajectory (QCT) method for NH(X<sup>3</sup>Σ<sup>-</sup>)+H(<sup>2</sup>S) reactions on their own high-quality potential energy surface [5]. At the same time, Poveda and Varandas reported a realistic global potential energy surface from double many-body expansion (DMBE) at the MRCI/aug-cc-pVQZ level [26]. Chu et al. investigated the time-dependent wave packet (TDWP) calculations for N+H<sub>2</sub> and N+D<sub>2</sub> reactions on this PES [9, 10]. Han and co-workers have calculated reaction kinetics employing the QCT and quantum mechanics methods on DMPE PES for H+NH reaction [27]. Akpınar et al. [11] and Defazio et al. [25] have presented the QM, QCT results and made comparisons with experimental results for the NH (a<sup>1</sup> Δ, v= 0,1)+H(<sup>2</sup>S) reaction. Quantum mechanical wave package calculations for H + ND reactions were performed by different groups using CS and CC methods [9-25]. Importantly, the influence RT coupling on NH<sub>2</sub> system was investigated in detail by the same

\* Corresponding author:

E-mail ([ssurucu@firat.edu.tr](mailto:ssurucu@firat.edu.tr))

groups. Comparing with current NH + H results, Defazio et al. [14] have pointed out the isotopic effects, which depend on the D and H masses. Banares et al. [28], Tanis[29] and Li et al. [18] have investigated the N + H<sub>2</sub> and H + DN reactions and their isotope variance, respectively, using TDWP and CS and CC methods, and explained the role of intermolecular isotope effects on reaction kinetics.

In this work, the time-dependent wave packet calculations were used to investigate a quantum dynamics study of the H+ND / H+NT reactions (for two reactive channels defined as ND (NT) +H→NH+D (T) exchange channel and ND (NT)+H→N+HD (HT) depletion channel), via real wave packet [30, 31], flux analysis method [32] and Centrifugal Sudden approximation. The two channels above are distinguished by comparing the internuclear distances of the product ND (NT) and HD (HT). The calculations have been carried out for the initial vibration quantum state ( $v_0=0$ ), the initial rotational states ( $j_0=2,3,4,5$ ), the total angular momentum quantum number ( $J$ ) up to 40 to get the reaction probabilities, the cross-sections, the rate constants. The main aims of the calculations are an investigation of the rotational effect on reaction system and explain the isotope effect by comparing the theoretical results available for H+ND /NT reactions.

## 2. Theory and Calculations

In this section, the TDWP method has been explained in terms of a mathematical formula, which is also well documented in the literature [31, 33-35]. This method is an effective and economical method for studying quantum reactive scattering dynamics. The triatomic Hamiltonian  $\hat{H}$  in reactant Jacobi Coordinates ( $R$ ,  $r$  and  $\theta$ ) can be written as,

$$\hat{H} = -\frac{\hbar^2}{2\mu_R} \frac{\partial^2}{\partial R^2} - \frac{\hbar^2}{2\mu_r} \frac{\partial^2}{\partial r^2} + \frac{j(j+1)}{2\mu_r r^2} + \frac{J(J+1)-K^2}{2\mu_R R^2} - \frac{1}{2\mu_R R^2} [J_+ J_- + J_- J_+] + V(R, r, \theta) \quad (1)$$

where  $R$  is the distance between atom and the center of mass of a molecule,  $r$  is the molecule bond length,  $\theta$  is the angle between  $R$  and  $r$  vectors,  $\mu_R$  is reduced the mass of the atom-molecule system along  $R$  coordinate, and  $\mu_r$  is the reduced mass of the diatomic molecule. In addition,  $J$  and  $j$  are the total angular momentum operator and rotational angular momentum operator, respectively [11, 16, 23, 25, 36, 37]. Moreover,  $J_+(J_-)$  and  $j_+(j_-)$  are the corresponding raising (lowering) operators which are known as Coriolis Coupling (CC) terms [16, 23, 38]. Also,  $V(R, r, \theta)$  is the interaction potential of the system. The fifth term in the Eq. (1) couple different  $K$  values and their neglecting give rise to the CS approximation. Hence,  $K$  is a conserved quantity under CS

approximation. It is worth noting here that in the body-fixed frame, initial  $K$  is the initial magnetic rotational quantum number of the diatom and  $K$  varies in the range  $0 \leq K \leq \min(J, j)$  for a given  $J$  and  $j$ . The reaction probability is taken out by calculating the flux at a fixed surface of corresponding time-dependent part of wave function after propagating for enough length of time,

$$P_{v_0 j_0}^{J K_0}(E) = \frac{\hbar}{\mu_r} \text{Im} \left\langle \Phi_{v_0 j_0}^+(E) \left| \delta(r-r_0) \frac{\partial}{\partial r} \right| \Phi_{v_0 j_0}^+(E) \right\rangle \quad (2)$$

where  $v_0$ ,  $j_0$ , and  $K_0$  are the initial quantum numbers to indicate the initial rovibrational state and  $\Phi_{v_0 j_0}^+(E)$  denotes the time-independent full scattering wave function. Also  $r_0$  is the location where the flux analysis [32] is carried out. The  $J$ -dependent reaction probability is computed from the propagated wave packet as:

$$P_{v_0 j_0}^J(E_{\text{col}}) = \frac{1}{2J+1} \left[ P_{v_0 j_0}^{J p K_0}(E_{\text{col}}) + 2 \sum_{K=1}^{\infty} P_{v_0 j_0}^{J p K_0}(E_{\text{col}}) \right] \quad (3)$$

where,  $p = \pm$  is the parity;  $E_{\text{col}}$  is equal to the difference between the total energy ( $E$ ) and the initial rovibrational energy ( $\epsilon_{v_0 j_0}$ ) of the diatomic molecule. Using the obtained reaction probabilities for all  $J$  values, the initial state-selected reaction cross-sections can be calculated by the following expression:

$$\sigma_{v_0 j_0 K_0}(E_{\text{col}}) = \frac{\pi}{2\mu_R E_{\text{col}} / \hbar^2} \sum_J (2J+1) \sum_{K=K_0}^{\infty} P_{v_0 j_0}^J(E_{\text{col}}) \quad (4)$$

Finally, the initial state specified rate constant can be obtained using the Boltzmann weight average of the cross-sections over the collision energy,

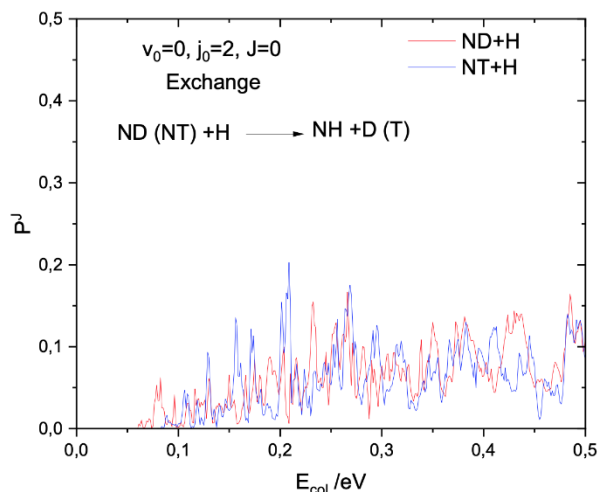
$$k_{v_0 j_0}(T) = \left( \frac{8}{\pi \mu_R k_B^3 T^3} \right)^{1/2} \int_0^{\infty} dE_{\text{col}} E_{\text{col}} e^{-E_{\text{col}}/k_B T} \sigma_{v_0 j_0 K_0}(E_{\text{col}}) \quad (5)$$

where  $T$  is the absolute temperature and  $k_B$  is the Boltzmann constant.

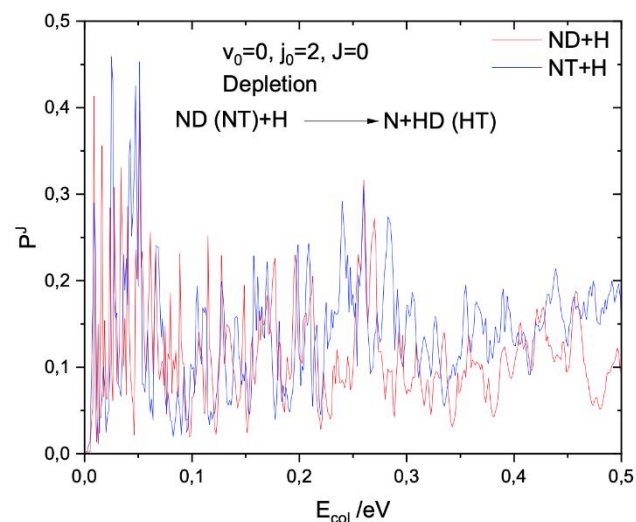
## 3. Results and Discussion

Figure 1 and Figure 2 show the reaction probabilities as a function of collision energy for the exchange and depletion channels of the ND+H and NT+H reactions. It can be seen from both Figure 1 and Figure 2 that the behavior of the reaction probabilities for both channels is rather different. The excited potential energy surface NH<sub>2</sub> does not have a barrier of the reaction pathway for both reaction channels. As shown in Figure 1, ND+H and NT+H reactions have a threshold. This threshold energy corresponds to quantum mechanical endothermicity which is the difference between the collision energies of the reactants and products and the threshold value for the NT + H reaction is greater

than that of the ND + H reaction. As shown in Figure 2, all the reaction probabilities of the depletion channels have not a threshold, due to barrierless and exothermic reaction properties and these probabilities for depletion channel are higher than the exchange channel. Generally, both reaction probabilities show a sharp oscillatory structure. These structures explain the influence of the deep and wide wells in the potential energy surface on the reaction kinetics.



**Figure 1.** The reaction probabilities for the exchange channel as a function of collision energy ( $E_{col}$ ).



**Figure 2.** The reaction probabilities for the depletion channel as a function of collision energy ( $E_{col}$ )

The reaction probabilities for exchange and depletion channels of both ND+H and NT+H reactions are demonstrated for different total angular momentum ( $J=5,10,15,20,30$ ) and the initial rotation state ( $j_0 = 2$ ) in Figure 3 and Figure 4, respectively. All the calculated reaction probabilities show a threshold value and the reaction threshold energies are greater in the larger total angular momentum quantum number. This shift in threshold energy is a result of the centrifugal potential

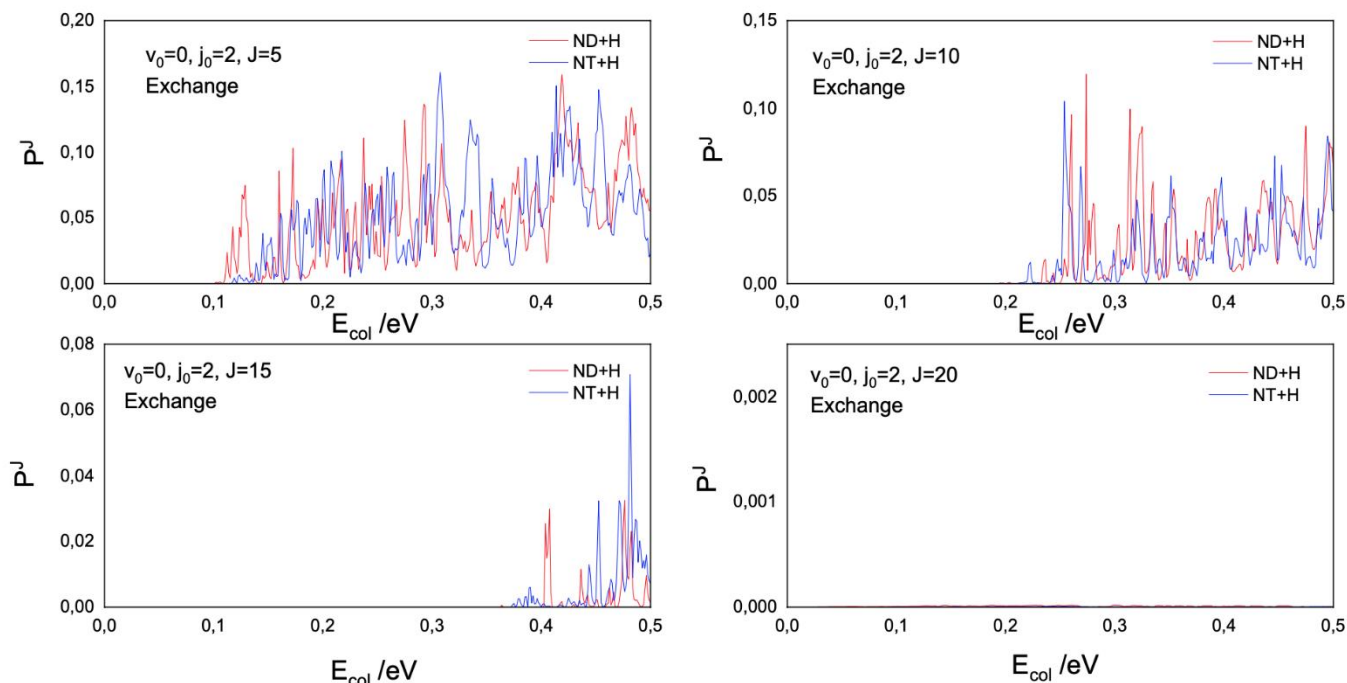


**Figure 3.** Reaction probabilities of exchange reaction channels for different total angular momentum and for the initial rotation states ( $j_0 = 2$ )

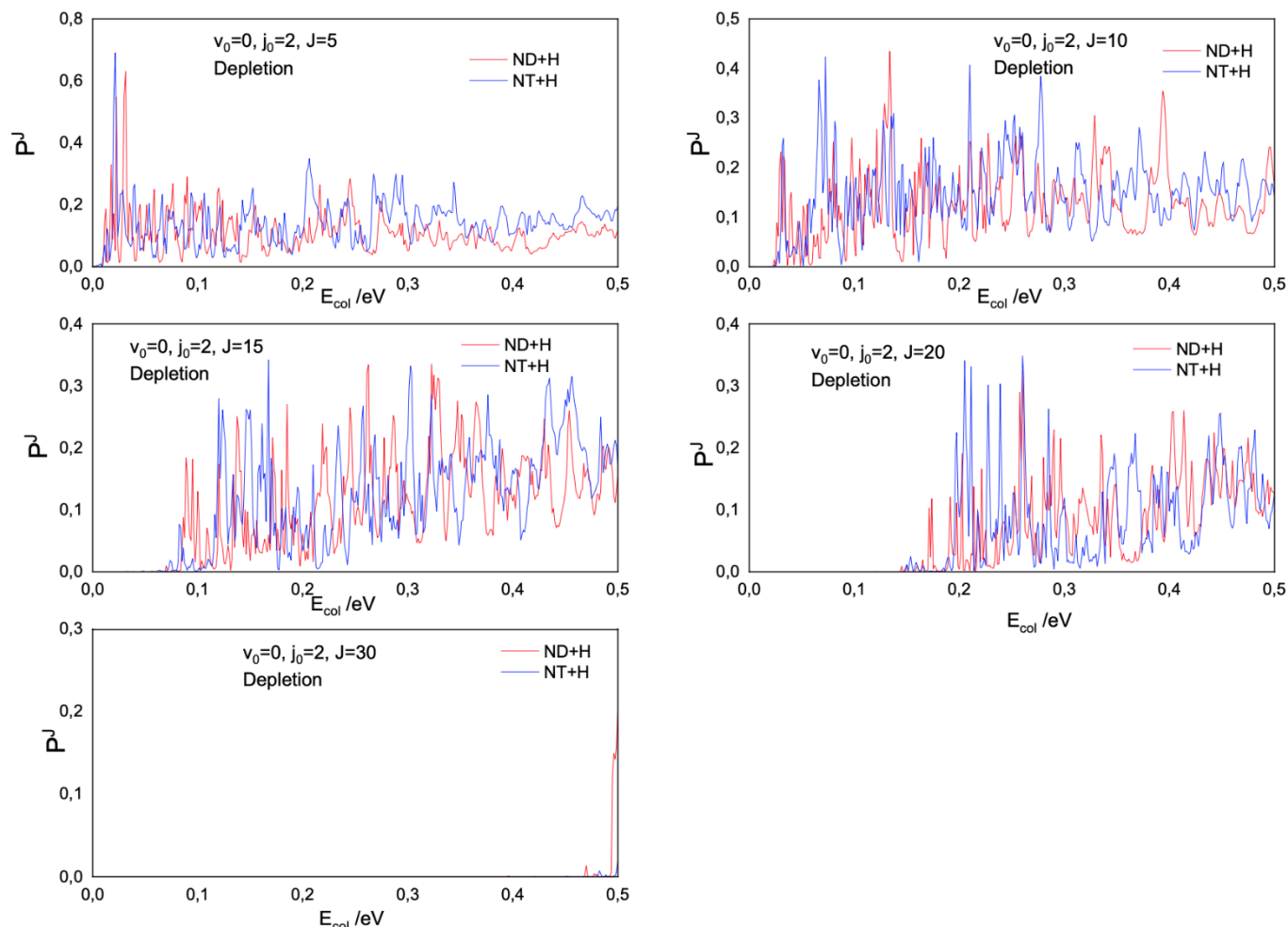
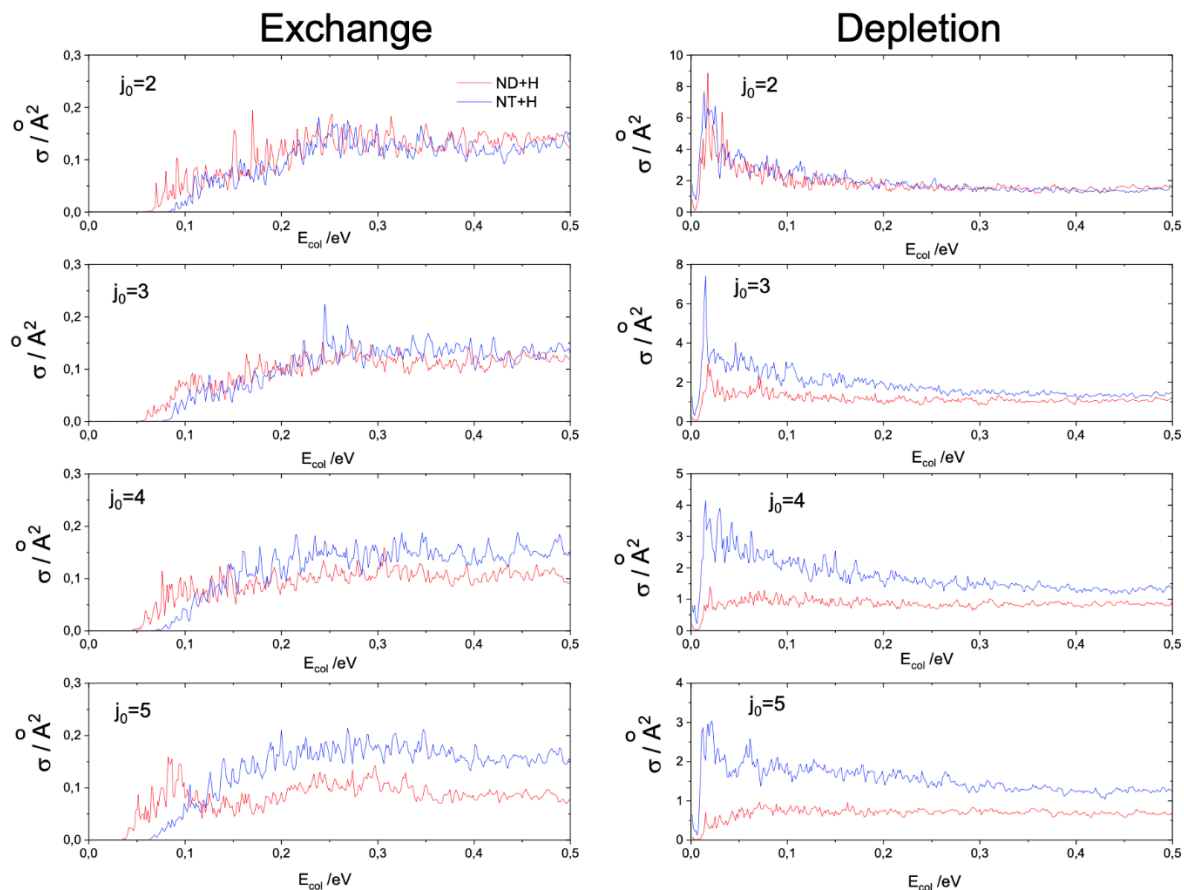


**Figure 4.** Reaction probabilities of depletion reaction channels for different total angular momentum and for the initial rotation states ( $j_0 = 2$ )

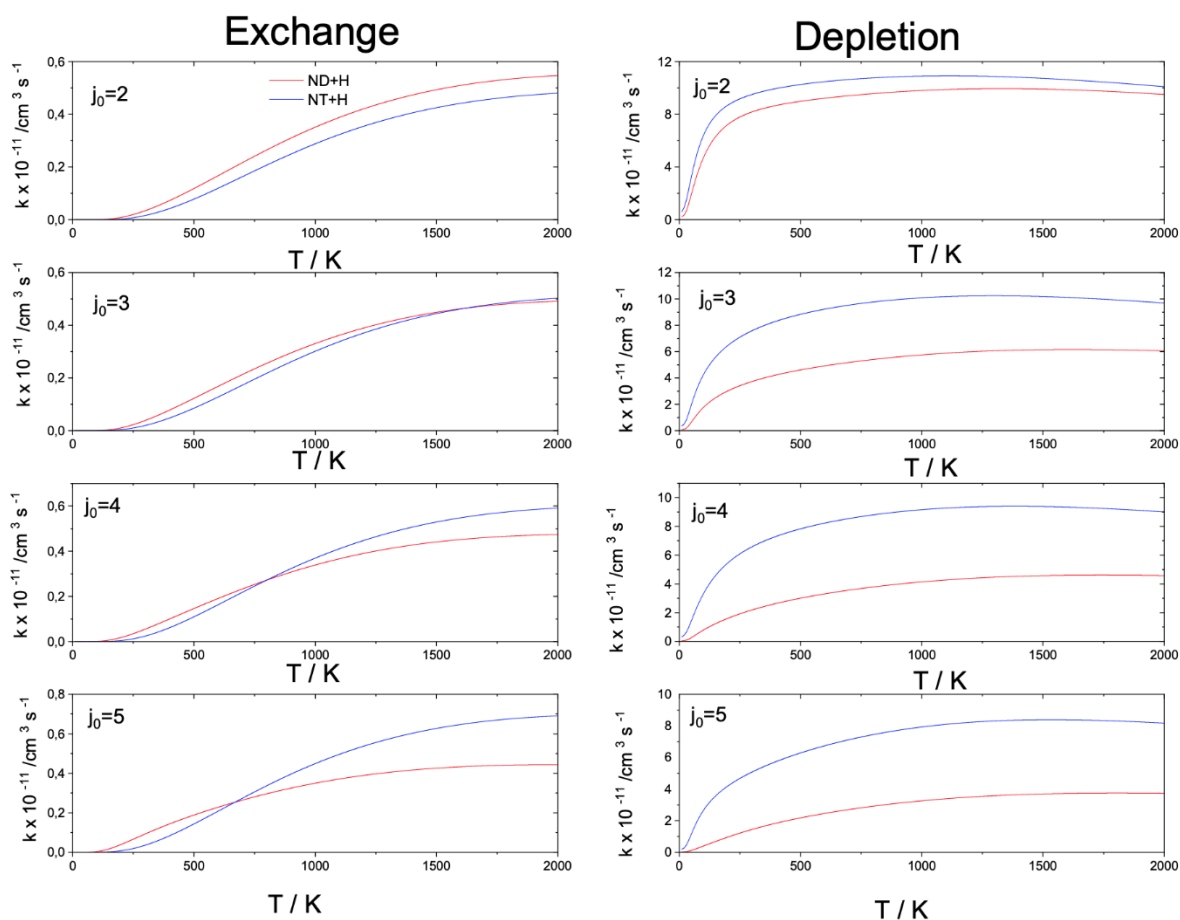
barrier. This barrier increases with increasing the value of angular momentum  $J$  [11, 16, 29]. Also, the reaction probabilities are not available for the exchange reaction channel of the ND+H and NT+H reactions at  $J \geq 20$  quantum state, but in the depletion channel of the reactions, the probability values are obtained at larger  $J$  values. The reason is that the masses of hydrogen, deuterium, and tritium isotope atoms displaced in the exchange reaction channel are very close to each other and the reaction process is short. In the depletion reaction channel, the long-lived of the intermediate complex which will form the new products oversees the probability formation at  $J \geq 20$  values.

Figure 5 shows the energy dependence of the integral cross sections for all the reactions. For the endothermic exchange reaction, the cross-sections show a threshold value in all quantum states indicated. As in the probability values, the threshold values of the NT + H reaction in the cross-sections are greater than ND+H reaction and then the cross-sections increase as the energy increases for all reactions. The cross-sections calculated for the exothermic depletion reaction show a definite increase in low collision

energy values and a decrease in high energy values. In addition, the role of isotope effect between ND+H and NT+H reactions is seen obviously in the quantum states in the figures. Because the PES has a deep well, the reaction channels have a reaction intermediate complex. Comparing to the ND+H reaction, the NT+H reaction has a larger mass; therefore, it is easier to be trapped in the deep well. So, the NT+H reaction is expected to have higher reactivity than ND+H reaction. This is confirmed by the results of reaction probabilities (Figures 1 and 2) and cross-sections (Figure 5). Reaction probabilities and cross-sections show clear D/T - isotopic and H-tunnel effects, associated with the heavier D/T mass. Because the lighter H/D atoms create a high tunneling effect [14]. However, the cross-sections are dependent on the initial rotational states. As can be seen from Figure 5, cross-sections decrease with increasing the initial rotational quantum number  $j_0$  for the ND+H and NT+H depletion reactions. For the exchange reaction, magnitudes of cross-sections increase with increase in  $j_0$  and the threshold energy of the reaction move to lower values as the rotational excitation increases.



**Figure 5.** Comparison between the cross-sections for different initial rotation quantum numbers for ND+H and NT+H reactions.



**Figure 6.** Comparison between the rate constant for different initial rotation quantum numbers for ND+H and NT+H reactions.



Reaction rate constants for exchange and depletion channels of ND + H and NT + H reactions depends on initial rotation quantum states are shown in Figure 6. For the exchange reaction, although the ND + H reaction is more reactive at lower temperatures, the NT + H reaction rate constant value is larger at higher temperatures. Differences in exchange channel rate constants at low temperatures result from the Maxwell- Boltzmann distribution at the quantum states of the molecules. For the depletion reaction, the rate constant values of the NT + H reaction are greater than the ND + H reaction at all specified quantum states and at all temperature values.

#### 4. CONCLUSIONS

In this study, initial- state- resolved reaction probabilities were calculated for ND+H and NT+H reaction systems on the modified NH<sub>2</sub> potential energy surface (PES) for  $\tilde{A}^2 A_1$  excited state. Theoretically calculated reaction probabilities, cross-sections and rate constants of ND+H and NT+H reactions have been shown clear D/T-isotopic and H-tunnel effects, associated with the heavier D/T mass. The influences of the initial rotational of the reactant on the reaction probabilities have been also studied. Rotational excitation of the reactive diatom (ND, NT) has different effects on both reaction channels. The cross section for depletion channel decreases with an increase in rotational state, the cross section for exchange channel increases with an increase in rotational state.

#### Acknowledgments

The author is indebted to Prof. Sinan Akpınar and Dr. Paolo Defazio for many stimulating discussions on quantum wave packet theory. The numerical calculations in this paper were performed on High Performance and Grid Computing Center (TR-Grid) machines at TUBITAK, ULAKBİM/TURKEY.

#### REFERENCES

1. Dodd, J.A., et al., *NH ( $X\ 3\Sigma^-$ ,  $v=1-3$ ) formation and vibrational relaxation in electron-irradiated Ar/N<sub>2</sub>/H<sub>2</sub> mixtures*. The Journal of chemical physics, 1991. **94**(6): p. 4301-4310.
2. Koshi, M., et al., *Reactions of N ( $4\ S$ ) atoms with NO and H<sub>2</sub>*. The Journal of chemical physics, 1990. **93**(12): p. 8703-8708.
3. Davidson, D. and R. Hanson, *High temperature reaction rate coefficients derived from N-atom ARAS measurements and excimer photolysis of NO*. International Journal of Chemical Kinetics, 1990. **22**(8): p. 843-861.
4. Suzuki, T., et al., *Reactions of N ( $2\ 2\ D$ ) and N ( $2\ 2\ P$ ) with H<sub>2</sub> and D<sub>2</sub>*. Journal of the Chemical Society, Faraday Transactions, 1993. **89**(7): p. 995-999.
5. Adam, L., et al., *Experimental and theoretical investigation of the reaction NH ( $X\ \Sigma^- 3$ ) + H ( $S\ 2$ ) → N ( $S\ 4$ ) + H<sub>2</sub> ( $X\ \Sigma\ g+ 1$ )*. The Journal of chemical physics, 2005. **122**(11): p. 114301.
6. Qu, Z.-W., et al., *Experimental and theoretical investigations of the reactions NH ( $X\ \Sigma^- 3$ ) + D ( $S\ 2$ ) → ND ( $X\ \Sigma^- 3$ ) + H ( $S\ 2$ ) and NH ( $X\ \Sigma^- 3$ ) + D ( $S\ 2$ ) → N ( $S\ 4$ ) + HD ( $X\ \Sigma\ g+ 1$ )*. The Journal of chemical physics, 2005. **122**(20): p. 204313.
7. Gogtas, F. and N. Bulut, *Quantum wave packet study of N ( $2D$ ) + H<sub>2</sub> reactive scattering*. International journal of quantum chemistry, 2006. **106**(4): p. 833-838.
8. Adam, L., et al., *Exploring Renner-Teller induced quenching in the reaction H ( $S\ 2$ ) + NH ( $a\ 1$ ): A combined experimental and theoretical study*. The Journal of chemical physics, 2007. **126**(3): p. 034304.
9. Chu, T.-S., K.-L. Han, and A.J. Varandas, *A quantum wave packet dynamics study of the N ( $2D$ ) + H<sub>2</sub> reaction*. The Journal of Physical Chemistry A, 2006. **110**(4): p. 1666-1671.
10. Chu, T.S., et al., *Accurate quantum wave packet study of the N ( $2D$ ) + D<sub>2</sub> reaction*. Chemical Physics Letters, 2007. **444**(4-6): p. 351-354.
11. Akpınar, S., et al., *Quantum dynamics of NH ( $a\ 1$ ) + H reactions on the NH  $2\ \tilde{A}^2 A_1$  surface*. The Journal of chemical physics, 2008. **129**(17): p. 174307.
12. Chu, T.-S., A.J. Varandas, and K.-L. Han, *Nonadiabatic effects in D++ H<sub>2</sub> and H++ D<sub>2</sub>*. Chemical Physics Letters, 2009. **471**(4-6): p. 222-228.
13. Defazio, P., et al., *Renner-Teller Quantum Dynamics of NH ( $a\ 1$ ) + H Reactions on the NH<sub>2</sub>  $\tilde{A}^2 A_1$  and  $\tilde{X}^2 B_1$  Coupled Surfaces*. The Journal of Physical Chemistry A, 2010. **114**(36): p. 9749-9754.
14. Defazio, P., et al., *Quantum dynamics of Renner-Teller and isotopic effects in NH ( $a\ 1$ ) + D ( $2\ S$ ) reactions*. Physical Chemistry Chemical Physics, 2011. **13**(18): p. 8470-8474.
15. Surucu, S., G. Tasmanoglu, and S. Akpınar, *A quantum wave packet study of the ND + D reaction*. Molecular Physics, 2012. **110**(14): p. 1525-1533.
16. Akpınar, S. and S.S. Hekim, *The effect of the Coriolis coupling on H + ND reaction: A time dependent wave packet study*. Chemical Physics Letters, 2013. **578**: p. 21-27.

17. Karabulut, E., et al., *The effect of initial rotation in the  $N(2D)+H_2 \rightarrow NH(3\Sigma^-)+H$  reaction*. Chemical Physics, 2014. **441**: p. 53-58.
18. Li, D., Y. Wang, and T. Wumaier, *Quantum and quasi-classical dynamics of reaction  $H+DN(v=0,1;j=0) \rightarrow HD+N$  and its isotopic variants*. The European Physical Journal D, 2016. **70**(8): p. 173.
19. Li, Z., et al., *Quantum and quasiclassical state-to-state dynamics of the  $NH+H$  reaction: Competition between abstraction and exchange channels*. The Journal of chemical physics, 2011. **134**(13): p. 134303.
20. Lin, S.Y., et al., *Non-Born–Oppenheimer State-to-State Dynamics of the  $N(2D)+H_2 \rightarrow NH(\tilde{X}3\Sigma^-)+H$  Reaction: Influence of the Renner–Teller Coupling*. The Journal of Physical Chemistry A, 2010. **114**(36): p. 9655-9661.
21. Santoro, F., C. Petrongolo, and G.C. Schatz, *Trajectory-Surface-Hopping Study of the Renner–Teller Effect in the  $N(2D)+H_2$  Reaction*. The Journal of Physical Chemistry A, 2002. **106**(36): p. 8276-8284.
22. Zhu, Z., et al., *Vibrational and rotational excitation effects of the  $N(2D)+D_2(X1\Sigma^+) \rightarrow ND(X3\Sigma^+)+D(2S)$  reaction*. Molecular Physics, 2018. **116**(9): p. 1108-1117.
23. Hekim, S. and S. Akpınar, *Investigation of coriolis coupling effect on the  $ND+D$  reaction*. Chemical Physics Letters, 2018. **706**: p. 87-92.
24. Hekim, S. and S. Akpınar, *Born oppenheimer and renner teller quantum dynamics of the  $ND+D$  reaction*. Chemical Physics Letters, 2019. **728**: p. 208-214.
25. Defazio, P., et al., *Relaxation of  $NH(a1\Delta, v=1)$  in Collisions with  $H(2S)$ : An Experimental and Theoretical Study*. The Journal of Physical Chemistry A, 2009. **113**(52): p. 14458-14464.
26. Poveda, L. and A. Varandas, *Repulsive double many-body expansion potential energy surface for the reactions  $N(4S)+H_2 \rightleftharpoons NH(X3\Sigma^-)+H$  from accurate ab initio calculations*. Physical Chemistry Chemical Physics, 2005. **7**(15): p. 2867-2873.
27. Han, B., et al., *Quasi-classical trajectory and quantum mechanics study of the reaction  $H(2S)+NH \rightarrow N(4S)+H_2$* . Chemical Physics Letters, 2010. **493**(4-6): p. 225-228.
28. Bañares, L., et al., *Influence of rotation and isotope effects on the dynamics of the  $N(D2)+H_2$  reactive system and of its deuterated variants*. The Journal of chemical physics, 2005. **123**(22): p. 224301.
29. Tanis, E., *Reactive scattering of an electronically-excited nitrogen atom with  $H_2$  and its isotopic variants:  $N(2D)+H_2/D_2/T_2$* . Computational and Theoretical Chemistry, 2016. **1081**: p. 38-43.
30. Gray, S.K. and G.G. Balint-Kurti, *Quantum dynamics with real wave packets, including application to three-dimensional ( $J=0$ )  $D+H_2 \rightarrow HD+H$  reactive scattering*. The Journal of chemical physics, 1998. **108**(3): p. 950-962.
31. Gogtas, F., et al., *Real wave packet and flux analysis studies of the  $H+F_2 \rightarrow HF+F$  reaction*. International Journal of Quantum Chemistry, 2012. **112**(11): p. 2348-2354.
32. Meijer, A.J., et al., *Flux analysis for calculating reaction probabilities with real wave packets*. Chemical physics letters, 1998. **293**(3-4): p. 270-276.
33. Kosloff, R., *Time-dependent quantum-mechanical methods for molecular dynamics*. The Journal of Physical Chemistry, 1988. **92**(8): p. 2087-2100.
34. Balakrishnan, N., C. Kalyanaraman, and N. Sathyamurthy, *Time-dependent quantum mechanical approach to reactive scattering and related processes*. Physics Reports, 1997. **280**(2): p. 79-144.
35. Tal-Ezer, H. and R. Kosloff, *An accurate and efficient scheme for propagating the time dependent Schrödinger equation*. The Journal of chemical physics, 1984. **81**(9): p. 3967-3971.
36. Aslan, E., et al., *Accurate Time-Dependent Wave Packet Study of the  $Li+H_2$  Reaction and Its Isotopic Variants*. The Journal of Physical Chemistry A, 2011. **116**(1): p. 132-138.
37. Poirier, B., *Analytical treatment of Coriolis coupling for three-body systems*. Chemical physics, 2005. **308**(3): p. 305-315.
38. Defazio, P. and C. Petrongolo, *Coriolis coupling effects on the initial-state-resolved dynamics of the  $N(D2)+H_2 \rightarrow NH+H$  reaction*. The Journal of chemical physics, 2007. **127**(20): p. 204311.